Journal of Solid State Chemistry **168,** 608–615 (2002)
doi:10.1006/jssc.2002.9758

Structures and Transport Properties of New Molecular Conductors Based on TMEO-ST-TTP

Yohji Misaki,*[,1] Masateru Taniguchi,* Kazuyoshi Tanaka,* Kazuo Takimiya,† Atsushi Morikami,† Tetsuo Otsubo,† and Takehiko Mori‡

*Department of Molecular Engineering, Graduate School of Engineering, Kyoto University, Yoshida, Kyoto 606-8501, Japan; †Department of Applied Chemistry, Faculty of Engineering, Hiroshima University, Higashi-Hiroshima 739-8527, Japan; and ‡Department of Organic and Polymeric Materials, Graduate School of Science and Engineering, Tokyo Institute of Technology, O-okayama, Tokyo 152-8552, Japan

Received January 15, 2002; in revised form May 2, 2002; accepted May 14, 2002

Several radical cation salts based on TMEO-ST-TTP (2-[4,5-bis(methylthio)-1,3-diselenol-2-ylidene]-5-(4,5-ethylendioxy-1,3-dithiol-2-ylidene)-1,3,4,6-tetrathiapentalene) have been prepared. X-ray structure analyses of (TMEO-ST-TTP)$_2X$ ($X = PF_6$, AsF_6, TaF_6) reveal that they have the so-called β-type array of donors with dimerized stacks. A tight-binding band calculation suggests that the present salts have a quasi-one-dimensional Fermi surface. On the other hand (TMEO-ST-TTP)Au(CN)$_2$ has strongly dimerized one-dimensional electronic structure. (TMEO-ST-TTP)$_2X$ ($X = PF_6$, AsF_6, TaF_6) exhibit a high conductivity of $\sigma_{rt} = 10^0 - 10^1\,S\,cm^{-1}$, and retain metallic conductivity down to 4.2 K, while the tetrahedral (ReO_4^-) and linear (I_3^- and $Au(CN)_2^-$) anions give semiconductors. Thermoelectric power of (TMEO-ST-TTP)$_2PF_6$ shows *T*-linear temperature dependence characteristic of a metal.

Key Words: **radical cation salts; organic metal; π-electron donor; tetrathiapentalene; X-ray structure analysis; band calculation; electrical conductivity: thermoelectric power.**

1. INTRODUCTION

Considerable efforts have been devoted to the development of molecular materials exhibiting exotic electrical property (1). In particular, preparation of new molecular superconductors has received considerable interest from various fields such as organic and physical chemistry, solid state physics and materials science (2). Although design of molecular superconductors has not been established yet, two promising strategies have been recognized to cause superconducting transition. One is realization of multidimesional electronic structure (at least quasi-one-dimensional) so that the metal-to-insulator transition (Peierls transition), to which one-dimensional metals are inherently subject (3), can be suppressed. The other is construction of strongly electron-correlated system by increase of on-site Coulomb repulsion or by narrowing bandwidth against stable metals down to low temperature because it has been recently pointed out that superconducting state lies between metal and antiferromagnetic Mott insulating state (4). In the search for molecular metals stable down to low temperatures, we have synthesized tetrathiapentalene-type donor 2,5-bis(1,3-dithiol-2-ylidene)-1,3,4,6-tetrathiapentalene (BDT-TTP) (5), and have reported that BDT-TTP and its derivatives afford a large number of radical cation salts showing metallic conducting behavior down to low temperatures (≤ 4.2 K) (6–12). It has been found that conducting materials based on BDT-TTP derivatives with various substituents also form two-dimensional conducting layer thanks to side-by-side interaction through sulfur atoms in the π-electron framework. It is contrastive that TTF derivatives need chalcogene-based substituents such as ethylenedithio group (13). BDT-TTP itself has a tendency to form the so-called β-type packing with uniform donor stacks, resulting in significant stabilization of metallic state down to low temperatures. In order to destabilize metallic state and to cause superconducting transition eventually, introduction of bulky groups on BDT-TTP framework is promising. Among a large number of BDT-TTP derivatives synthesized so far, several BDT-TTP derivatives with methylthio groups have been found to afford metallic radical cation salts down to low temperatures (8, 14). It is noted that 4,5-bis(methylthio)-4′,5′-ethylendioxy-TTP (TMEO-TTP) has yielded many radical cation salts, which retain metallic conductivity down to liquid helium temperature (12). Their crystal structures have not been unfortunately well-characterized due to shortage of good-quality crystals. Just three kinds of

[1] To whom correspondence should be addressed. Fax: +81 75 771 0172. E-mail: misaki@mee3.moleng.kyoto-u.ac.jp.

0022-4596/02 $35.00

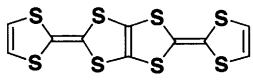

BDT-TTP

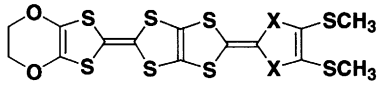

X = S, TMEO-TTP
X = Se, TMEO-ST-TTP

CHART 1.

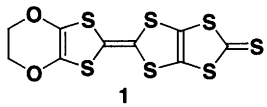

1

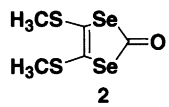

2

CHART 2.

radical cation salts, $(TMEO\text{-}TTP)_2Au(CN)_2$ (14), (TMEO-TTP)$AuBr_2 \cdot$(THF) (15), and $(TMEO\text{-}TTP)_3SbF_6$ (16) have been determined by their crystal structures. Among them, only the $Au(CN)_2$ salt shows metallic behavior, and the others are semiconductors from room temperature. Although $(TMEO\text{-}TTP)_2Au(CN)_2$ has uniform pseudo-stack, the other salts have dimerized or trimerized face-to-face stacks. Therefore, development of molecular conductors based on TMEO-TTP and its analogous donor is of interest to explore 2:1 metals with dimerized structures, which bring narrow bandwidth with half-filled band as is observed in many BEDT-TTF superconductors. In this paper, we report structures and properties of organic conductors based on a selenium analogue of TMEO-TTP, TMEO-ST-TTP, where is 2-[4,5-bis(methylthio)-1,3-diselenol-2-ylidene]-5-(4,5-ethylenedioxy-1,3-dithiol-2-ylidene)-1,3,4,6-tetrathiapentalene (17) (Charts 1 and 2).

2. EXPERIMENTAL METHODS

2.1. Synthesis

2.1.1. Synthesis of 2-[4,5-Bis(methylthio)-1,3-diselenol-2-ylidene]-5-(4,5-ethylenedioxy-1,3-dithiol-2-ylidene)-1,3,4,6-tetrathiapentalene (TMEO-ST-TTP)

To a suspension of 2-(4,5-ethylenedioxy-1,3-dithiol-2-ylidene)-1,3,4,6-tetrathiapentalen-5-thione (**1**) (250 mg, 0.68 mmol) and 4,5-bis(methylthio)-1,3-diselenol-2-one (**2**) (209 mg, 0.68 mmol) in toluene (15 mL) was added trimethylphosphite (7 mL) at 80°C under argon atmosphere. The reaction mixture was stirred for 2 h at 80°C, and then cooled down to room temperature. The resultant reddish brown precipitate was filtered off, washed with *n*-hexane, and then dried in vacuo. The residue was column chromatographed on silica gel with CS_2 as the eluent to afford TMEO-ST-TTP (135 mg, 0.22 mmol) as dark red crystals in 32% yield. mp 215–216°C (dec.); IR(KBr) 3440, 2917, 1651, 1434, 1162 cm^{-1}; ^1H NMR (CS_2–C_6D_6) δ 4.25 (s, 4 H), 2.44 (s, 6 H) ; MS *m/z* 626 (M^+); Anal. Calcd for $C_{14}H_{10}O_2S_8Se_2$: C, 26.92; H, 1.61. Found: C, 27.01; H, 1.48.

2.1.2. Preparation of Radical Cation Salts of TMEO-ST-TTP

Black needle- or plate-like crystals were electrochemically grown at 50°C in chlorobenzene or 1,2-dichloroethane (17 mL) containing ethanol (1 mL, ca. 5%) in the

TABLE 1
Crystallographic Data of TMEO-ST-TTP Salts

Compound	$(TMEO\text{-}ST\text{-}TTP)_2TaF_6$	$(TMEO\text{-}ST\text{-}TTP)_2PF_6$	$(TMEO\text{-}ST\text{-}TTP)_2AsF_6$	$(TMEO\text{-}ST\text{-}TTP)Au(CN)_2$
Chemical formula	$C_{28}H_{20}O_4S_{16}Se_4TaF_6$	$C_{28}H_{20}O_4S_{16}Se_4PF_6$	$C_{28}H_{20}O_4S_{16}Se_4AsF_6$	$C_{16}H_{10}O_2S_8Se_2AuN_2$
Molecular weight	1544.20	1394.22	1438.18	873.63
Crystal system	Monoclinic	Triclinic	Triclinic	Monoclinic
Space group	$P2_1/n$	$P\bar{1}$	$P\bar{1}$	$P2_1/n$
a (Å)	7.445(2)	8.205(5)	8.238(4)	12.996(7)
b (Å)	40.108(10)	19.074(6)	19.169(7)	8.293(7)
c (Å)	8.177(3)	7.456(3)	7.440(3)	22.425(7)
α (deg)		91.67(3)	92.27(4)	
β (deg)	104.20(3)	103.80(4)	103.73(4)	97.03(3)
γ (deg)		83.14(3)	82.86(4)	
V (Å^3)	2367(1)	1125.1(9)	1132.4(8)	2398(2)
Z	2	1	1	4
D_c (g cm^{-3})	2.166	2.103	2.109	2.419
μ (cm^{-1})	61.58	41.37	47.64	99.07
R	0.072	0.050	0.078	0.049
R_w	0.082	0.054	0.091	058
Reflections measured	4756	3965	5200	5503
Reflections used	2308 ($I > 3\sigma(I)$)	1613 ($I > 3\sigma(I)$)	1847 ($I > 3\sigma(I)$)	2309 ($I > 3\sigma(I)$)

presence of the donor (2–3 mg) and the corresponding tetra-*n*-butylammonium salts (30–40 mg). The current was stepwisely changed from 0.2 to 0.7 μA during electrocrystallization (1–2 weeks) (18).

2.2. Physical Mesurements

2.2.1. X-Ray Diffractional Analyses

The black plate crystals were used for X-ray measurements at 296 K on a Rigaku AFC7R diffractometer equipped with graphite monochromated Mo$K\alpha$ radiation and a 12 kW rotating anode generator. Crystal data are shown in Table 1. Cell constants were determined from 20 well- centered reflections in the range $7.79 < 2\theta < 22.05°$. Intensity data were collected to a maximum 2θ value of 55° by the $\omega - 2\theta$ scan technique. After absorption correction was applied, the structure was solved by direct methods (SHELEX86) (19). The non-hydrogen atoms were refined anisotropically. Hydrogen atoms were included, but not refined.

2.2.2. Electrical Conductivity Measurement

The electrical conductivity was measured by the four-probe technique with low-frequency alternating current using a Huso Electro Chemical System HESS 994 Multichannel 4-terminal conductometer. Electrical contacts were achieved with gold paste.

2.2.3. Thermoelectric Power Measurement

The thermoelectric power was measured by attaching a single crystal to copper heat blocks with gold paste. The measurement was made along the crystal long axis in the temperature range 24–296 K.

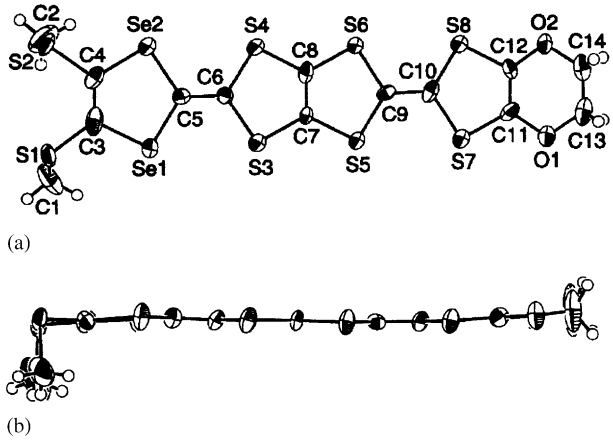

FIG. 1. (a) ORTEP drawing and atomic numbering scheme of TMEO-ST-TTP in (TMEO-ST-TTP)$_2$TaF$_6$ and (b) the side view.

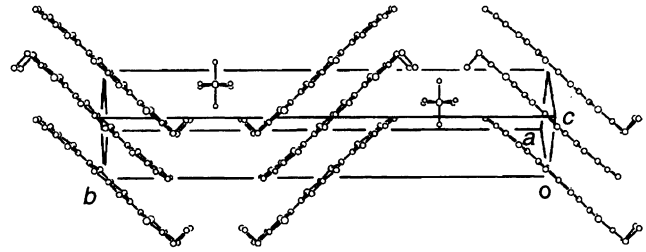

FIG. 2. Crystal structure of (TMEO-ST-TTP)$_2$TaF$_6$ projected onto the *ab* plane.

2.2.4. Band Calculation

The tight-binding band structure was calculated on the basis of the extend Hückel approximation, according to which the transfer integrals are assumed to be proportional to the intermolecular overlap integrals of frontier molecular orbitals. The basis set consisted of Slater-type orbital single-ζ quality for Se 4*s*, 4*p* and 4*d*, S 3*s*, 3*p* and 3*d*, C 2*s* and 2*p* and H 1*s* orbitals (20).

3. RESULTS AND DISCUSSION

3.1. Crystal Structures

Among the radical salts obtained so far, X-ray structure analyses of four kinds of salts, TaF_6^-, AsF_6^-, PF_6^- and $Au(CN)_2^-$ have been successful. Their crystallograhic data are summarized in Table 1.

(TMEO-ST-TTP)$_2$TaF$_6$: This salt crystallizes in the monoclinic system $P2_1/m$. One donor molecule is crystallographically independent which is located on a general position, whereas the octahedral TaF_6^- anion lies on a two-fold axis. Figure 1 shows ORTEP drawing of TMEO-ST-TTP molecule in this salt with atomic numbering scheme.

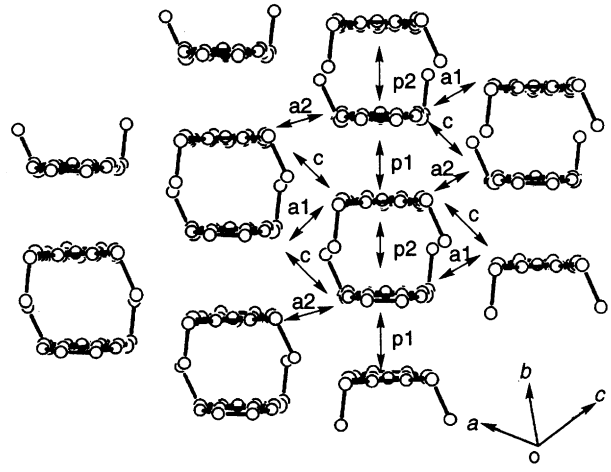

FIG. 3. Donor arrangement of (TMEO-ST-TTP)$_2$TaF$_6$ viewed along the donor long axis.

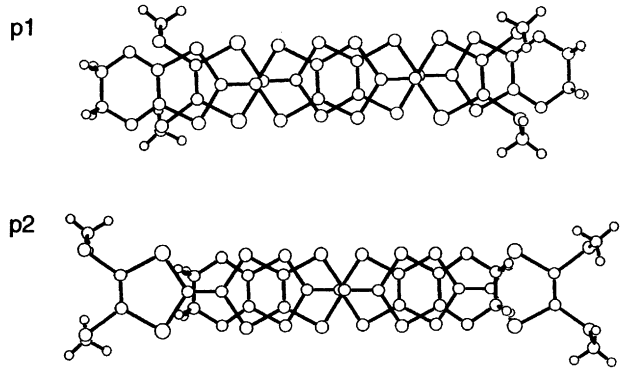

FIG. 4. Overlap modes of donor molecules in $(TMEO\text{-}ST\text{-}TTP)_2TaF_6$.

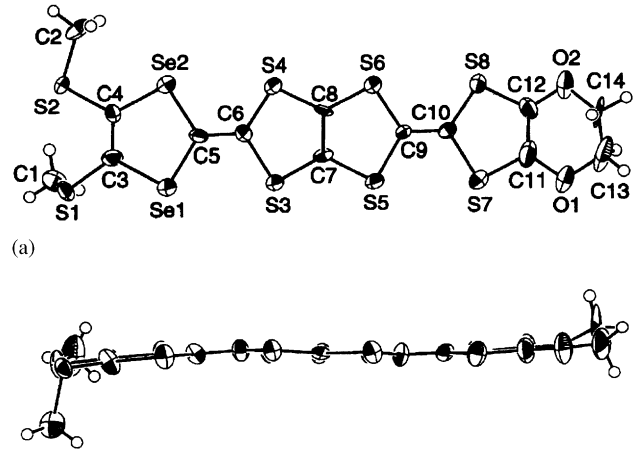

FIG. 6. (a) ORTEP drawing and atomic numbering scheme of TMEO-ST-TTP in $(TMEO\text{-}ST\text{-}TTP)Au(CN)_2$ and (b) the side view.

The molecule is completely planar except for two methyl groups, both of which stick up from the molecular plane. The crystal structure of $(TMEO\text{-}ST\text{-}TTP)_2TaF_6$ is shown in Fig. 2. A unit cell contains four donor molecules and two anions. The donors form conducting sheets along the *ac* plane, each of which is divided from the insulating layer composed of the anions. The neighboring donor layers are tilted in opposite directions to each other. The packing pattern of the donor molecules is the so-called β-type in BEDT-TTF conductors (Fig. 3) (21). The TMEO-ST-TTP molecules form a face-to-face stack with interplanar distances of 3.52 and 3.56 Å, respectively. There are two overlap modes in the stack (Fig. 4). Both modes are found to be the so-called ring-over-bond type; however, the slip distance along the donor long axis (D) is quite different from each other. That is, one of them corresponds to about a half of the 1,3-dithole ring ($p1$, $D = 1.6$ Å) as observed in well-overlapped stacks such as $(BDT\text{-}TTP)_2X$ ($X = SbF_6$, ClO_4, etc.) (6), while the other to a larger slip of about one and half of the 1,3-dithole ring ($p2$, $D = 4.9$ Å).

$(TMEO\text{-}ST\text{-}TTP)_2PF_6$ and $(TMEO\text{-}ST\text{-}TTP)_2AsF_6$: These two salts are isostructural with each other and crystallize in the triclinic system. The crystal structure of $(TMEO\text{-}ST\text{-}TTP)_2PF_6$ is shown in Fig. 5. A unit cell contains two donor molecules and one anion. One donor molecule is crystallographically independent which is located on a general position, whereas the octahedral PF_6^- anion lies on a center of inversion. The donors form conducting sheets along the *ac* plane, each of which is separated from the anion layer similar to $(TMEO\text{-}ST\text{-}TTP)_2TaF_6$. In these salts. however, two neighboring donor layers are tilted in the same direction unlike $(TMEO\text{-}ST\text{-}TTP)_2TaF_6$. In spite of the different crystal

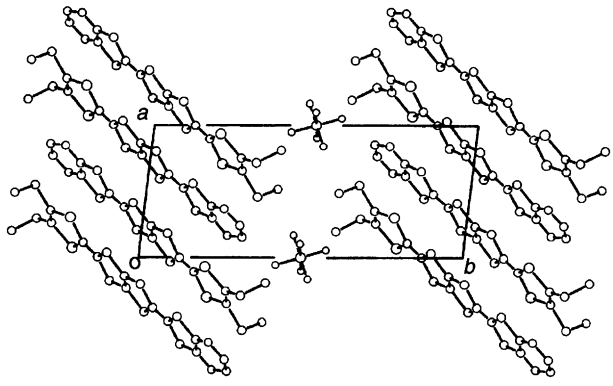

FIG. 5. Crystal structure of $(TMEO\text{-}ST\text{-}TTP)_2PF_6$ projected onto the *ab* plane.

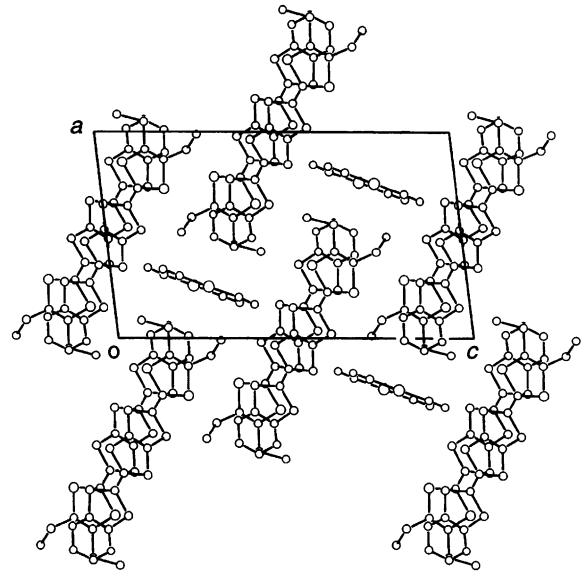

FIG. 7. Crystal structure of $(TMEO\text{-}ST\text{-}TTP)Au(CN)_2$ projected onto the *ab* plane.

system from the TaF_6^- salt, molecular structure of TMEO-ST-TTP and the packing patterns of the donors in a conducting sheet resemble each other. Namely, the array of the TMEO-TTP molecules is β-type, and the donors form a face-to-face stack with slip distances along the donor long axis of a half (1.7 Å) and one- half (5.0 Å) of the 1,3-dithiole rings, respectively.

(TMEO-ST-TTP)Au(CN)$_2$: One donor molecule and anion are crystallographically independent; therefore, the ratio of donor to anion is 1:1. It is in contrast that the corresponding all sulfur analogue TMEO-TTP is known to afford the 2:1 salt. The TMEO-ST-TTP molecule has a slightly folded structure at the S3–S4 position. The dihedral angle between Se1–Se2–S3–S4 and S3–S4–S5–S6 optimal planes is 3.6°. In contrast to the salts with octahedral anions, direction of bent methylthio groups is different from each other (Fig. 6). One of the methyl groups in the molecule overhangs from the molecular plane similar to the octahedral anion salts. On the other hand, the other is located in the molecular plane, whereas the other projects outside of the molecular long axis in the plane composed of the donor skeleton. Figure 7 shows the crystal structure of this salt. The TMEO-ST-TTP molecules form a column along the *b* direction. The $Au(CN)_2^-$ anion does not form layered structure, and is located in a cavity surrounded by four donor molecules in the *ac* plane. TMEO-ST-TTP molecules also form two-dimensional network in the *ac* plane; therefore, the donors are arranged as three dimensional at a glance. There are two overlap modes in the column similar to the octahedral anion salts. However, the degree of dimerization is quite different from each other. One of overlaps of the $Au(CN)_2^-$ salt is face-to-face stack with slip distance along the molecular long axis of 1.6 Å, while the other is largely slipped along both the molecular long (2.6 Å) and short axes (1.4 Å), respectively (Fig. 8).

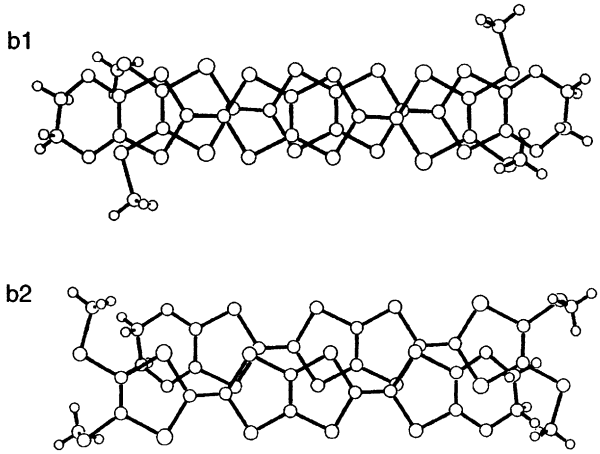

FIG. 8. Overlap modes of donor molecules in (TMEO-ST-TTP)Au(CN)$_2$.

3.2. Ovealap Integrals and Band Structures

(TMEO-ST-TTP)$_2$X (X = PF$_6$, AsF$_6$, TaF$_6$): The band parameters of TMEO-ST-TTP salts are summarized in Table 2. The differences of interplanar distances (z) in the stack are only 0.02–0.04 Å for the salts with octahedral anions. From the viewpoint of z values, the donors seem to be stacked uniformly; however, the donors are electronically dimerized along the stacking direction because the slip distances along the donor long axis (D) are quite different from each other (1.6–1.7 Å for $p1$, 4.9–5.0 Å for $p2$). The ratio of the calculated overlap integrals ($p1/p2$) is 1.9–2.3 for those salts. Figure 9 shows the energy dispersion and Fermi surface calculated by a tight-binding calculation. Because a conducting sheet in a unit cell contains two donor molecules, there are two bands, which are separated from each other due to strong dimerization along the stacking direction. The bandwidths of the upper bands for these salts are 0.51–0.55 eV and the energy gaps are 0.05–0.08 eV, respectively. As a result, upper bands of the present salt are effectively half-filled. Although the interstack overlap integrals of the salts with octahedral anions are 20–30% as large as those of larger intrastack ones ($p1$), the calculated Fermi surface is open, reflecting the quasi-one-dimensinality along the stacking ($a+c$)-axis.

(TMEO-ST-TTP)Au(CN)$_2$: One of the intrastack overlap integrals $b2$ ($S = -6.9 \times 10^{-3}$) is quite small owing to large slips along the donor long and short axes. In contrast, another intrastack overlap $b1$ ($S = 45.5 \times 10^{-3}$) is a little larger than those of the salts with octahedral anions ($S = 36.2-38.1 \times 10^{-3}$) because of shorter interplanar distance ($z = 3.43$ Å) than those of octahedral salts ($z = 3.52-3.56$ Å). Dimerization of the donors along the stack is significantly strong ($b1/b2 = 6.6$) compared to the other TMEO-ST-TTP salts as a result ($p1/p2$ = ca. 2). On the other hand, interstack interactions along the c-axis are significantly small because the donors in the neighboring column tilt in the opposite directions (Fig. 10). Furthermore, there is no overlap along the a-axis as the donors are extremely slipped along the donor long axis. Therefore, this salt may be regarded as a one-dimensional system in spite

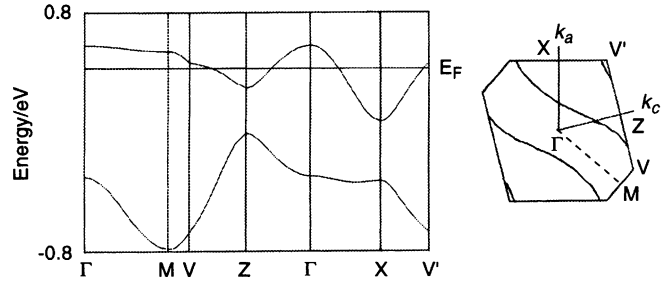

FIG. 9. The energy dispersion and Fermi surface of (TMEO-ST-TTP)$_2$TaF$_6$.

TABLE 2
Band Parameters of TMEO-ST-TTP Salts

Materials	z (Å)	D (Å)	Intrastack overlap ($\times 10^{-3}$)	Interstack overlap ($\times 10^{-3}$)	Bandgap (eV)	W_u(eV)	$W_u/\Delta E$
$(TMEO\text{-}ST\text{-}TTP)_2PF_6$	3.52 (p1)	1.7 (p1)	36.2 (p1)	−6.8 (a1)	0.05	0.55	0.76
	3.50 (p2)	5.0 (p2)	19.4 (p2)	−4.8 (a2)			
				−7.0 (c)			
$(TMEO\text{-}ST\text{-}TTP)_2AsF_6$	3.54 (p1)	1.7 (p1)	38.1 (p1)	−5.0 (a1)	0.08	0.53	0.70
	3.51 (p2)	5.0 (p2)	16.9 (p2)	−4.1 (a2)			
				−7.8 (c)			
$(TMEO\text{-}ST\text{-}TTP)_2TaF_6$	3.56 (p1)	1.6 (p1)	36.4 (p1)	−4.6 (a1)	0.07	0.51	0.70
	3.52 (p2)	4.9 (p2)	19.1 (p2)	−7.0 (a2)			
				−6.8 (c)			
$(TMEO\text{-}ST\text{-}TTP)Au(CN)_2$	3.43 (b1)	1.6 (b1)	45.5 (b1)	−0.5 (c)	0.72	0.15	0.16
	3.61 (b2)	2.6, 1.4[a] (b2)	-6.9 (b2)	0.5 (p1)			
				0.2 (p2)			
$(TMEO\text{-}ST\text{-}TTP)_2ClO_4(DCE)$ (17a)	3.50 (c1)	4.7 (c1)	18.0 (c1)	−8.7 (a1)	0.22	0.43	0.58
	3.43 (c2)	1.7 (c2)	36.9 (c2)	−10.3 (a2)			
				−7.6 (a3)			

[a] Slip distance along the donor short axis.

of the three-dimensional molecular arrangement at a glance. The small overlap integrals other than $b1$ result in a narrow upper band ($W_u = 0.15$ eV) and a large bandgap of 0.72 eV. Considering the ratio of donor to anion is 1:1, this salt is concluded to be a band insulator (Fig. 11).

3.3. Transport Properties

The electrical conductivity of the cation radical salts based on TMEO-ST-TTP was measured using the four-probe technique. Their electrical properties are summarized in Table 3. The salts with octahedral anions (PF_6^-, AsF_6^-, TaF_6^-) show high conductivity of $\sigma_{rt} = 10^0 - 10^1\,S\,cm^{-1}$, and exhibit metallic temperature dependence down to 4.2 K (Fig. 12). Although the band calculation indicates that these salts have quasi-one-dimensional Fermi surface open with respect to the stacking direction, the metal-to-insulator transition derived from Peierls instability is fortunately suppressed thanks to relatively strong side-by-side interaction (20–30% of the larger intrastack interaction, $p1$). On the other hand, the tetrahedral (ReO_4^-) and linear anions ($Au(CN)_2^-$ and I_3^-) have afforded semiconductors, although the I_3^- salt shows high conductivity of $\sigma_{rt} = 30\,S\,cm^{-1}$. The room temperature conductivity of the $Au(CN)_2^-$ salt is low ($\sigma_{rt} = 10^{-3}\,S\,cm^{-1}$) in accordance with the result of band calculation, that is, it is a band insulator.

Among the salts obtained so far, thermoelectric power of the $(TMEO\text{-}ST\text{-}TTP)_2PF_6$ was measured. The thermoelectric power is a positive value of $38\,\mu V\,K^{-1}$ at room temperature, and shows T-linear in the whole temperature range as is observed in a metal (Fig. 13) (22). The thermoelectric power of a tight-binding one-dimensional band is given as

$$S = \frac{\pi^2 k_B^2 T}{6et} \frac{\cos(1/2\pi\rho)}{1 - \cos^2(1/2\pi\rho)}.$$

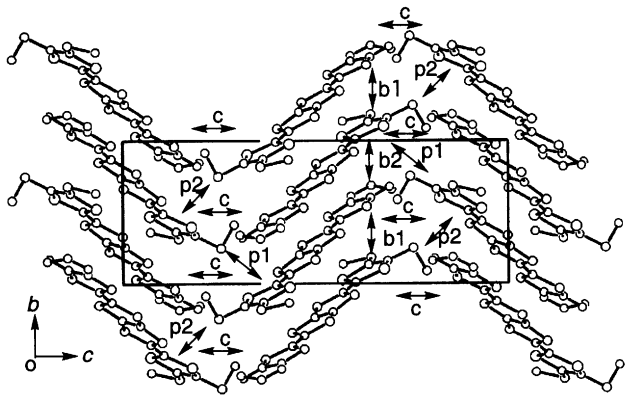

FIG. 10. Donor arrangement of $(TMEO\text{-}ST\text{-}TTP)Au(CN)_2$ projected onto the bc plane.

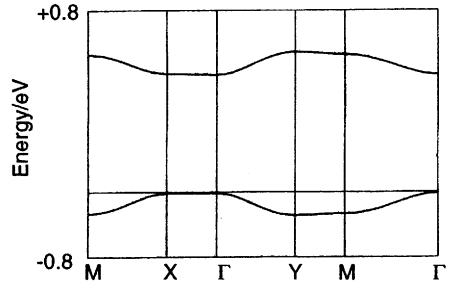

FIG. 11. The energy dispersion of $(TMEO\text{-}ST\text{-}TTP)Au(CN)_2$.

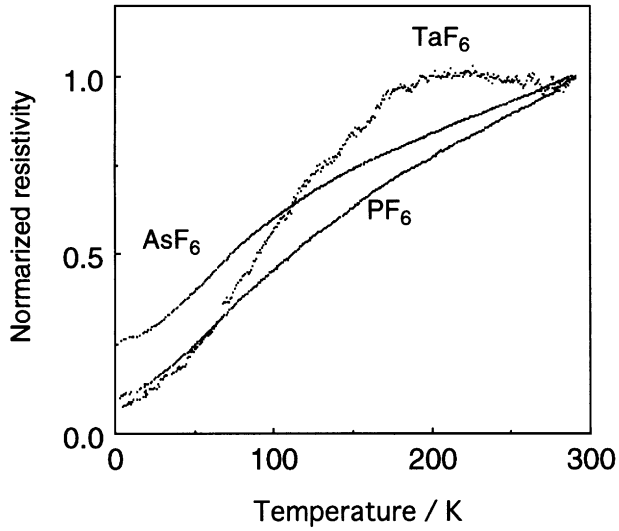

FIG. 12. Conducting behavior of metallic TMEO-ST-TTP salts.

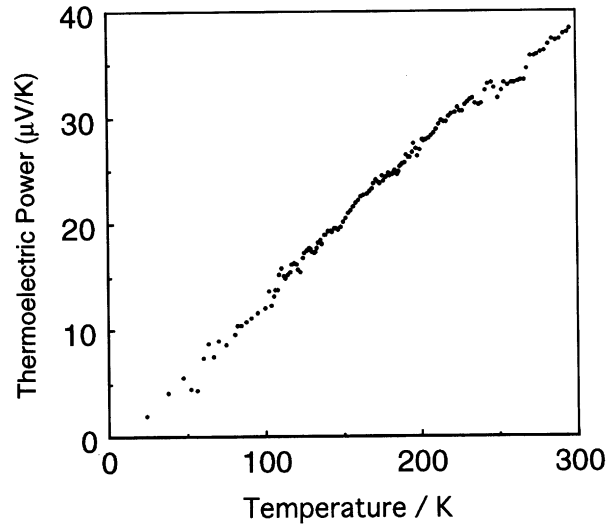

FIG. 13. Temperature dependence of the thermoelectric power of $(TMEO\text{-}ST\text{-}TTP)_2PF_6$.

From this equation, the bandwidth of this salt is calculated to be 0.56 eV. The small bandwidth estimated from the thermoelectric power, in comparison with the large bandwidth evaluated from the band calculation (1.8 eV), indicates importance of the correlation effect. This may be associated with the strong dimerization (Table 2). The conductivity, however, remains metallic down to low temperatures, and the thermoelectric power is T-linear, probably on account of the large overall bandwidth.

3.4. Comparison of $(TMEO\text{-}ST\text{-}TTP)_2X$ ($X = PF_6$, AsF_6, TaF_6) with $(TMEO\text{-}ST\text{-}TTP)_2ClO_4(DCE)$

In spite of resemblance of the donor packing pattern, TMEO-ST-TTP salts with octahedral anions and $(TMEO\text{-}ST\text{-}TTP)_2ClO_4(DCE)$ (17a) show significantly different conducting behavior from each other. Namely, octahedral anions afford stable metals down to low temperature, while ClO_4^- salt is a semiconductor from room temperature with low conductivity ($\sigma_{rt} = 0.07\,S\,cm^{-1}$, $E_a = 0.05$ eV) (17a). Komatsu et al. have reported that metallic or insulating state of 2:1 salts can be estimated from the ratio of the upper bandwidth (W_U) and the energy splitting (ΔE) defined by twice the intradimer transfer integrals (23, 24). That is, metallic conductivity could be realized if $W_U/\Delta E$ is large enough. In contrast, a $W_U/\Delta E$ smaller value than a threshold makes the material Mott insulator. The threshold for the BEDT-TTF salts has been estimated to be 1.0–1.1. On the other hand, ΔE values of the octahedral and ClO_4^- salts of TMEO-ST-TTP are almost the same. However, $W_U/\Delta E$ values (0.7–0.78) of the metallic octahedral anion salts are much larger than that of semiconduting ClO_4^- salt (0.58) because W_U values of the metallic octahedral anion salts (0.51–0.55 eV) are larger by ca. 0.1 eV compared with the ClO_4^- salt (0.43 eV). Therefore, it may be concluded that $(TMEO\text{-}ST\text{-}TTP)_2ClO_4(DCE)$ is a Mott insulator with a narrow effectively half-filled band, while the octahedral anion salts show metallic behavior thanks to relatively large W_U. The threshold between metal and Mott insulator

TABLE 3
Electrical Properties of TMEO-ST-TTP Salts ($TMEO\text{-}ST\text{-}TTP \cdot A_x$)

Anion	Solvent	Form	x^a	$\sigma_{rt}(S\,cm^{-1})^b$	
ReO_4^-	PhCl	Needle	1.3(Re)	0.9	$E_a = 0.056$ eV
	DCE	Plate	0.51(Re)	0.2	$E_a = 0.35$ eV
PF_6^-	PhCl	Plate	0.5(X)	30	Metallic down to 4.2 K
AsF_6^-	DCE	Plate	0.5(X)	40	Metallic down to 4.2 K
TaF_6^-	PhCl	Plate	0.5(X)	5	Metallic down to 4.2 K
I_3^-	PhCl	Needle	0.40(I)	30	$E_a = 0.015$ eV
$Au(CN)_2^-$	PhCl	Plate	1.0(X)	1×10^{-3}	$E_a = 0.17$ eV

[a] Determined by the energy dispersion spectroscopy from the ratio of sulfur and the elements designated in parentheses. X designates the value determined from the single-crystal X-ray structure analysis.

[b] Room temperature conductivity measured by four-probe technique on a single crystal.

for TMEO-ST-TTP salts may be estimated to be 0.6–0.7, which is about two-thirds as large as that of BEDT-TTF salts. In spite of such small $W_U/\Delta E$, corresponding to Mott insulating state for BEDT-TTF salts, TMEO-ST-TTP salts exhibit metallic conductivity probably due to small on-site Coulomb energy of TMEO-ST-TTP by extension of π-electron conjugation (twice as large as that of TTF) (25).

4. CONCLUSION

New molecular metals stable down to liquid helium temperature have been prepared from TMEO-ST-TTP and octahedral anions. Those salts have the so-called β-type donor packing with strongly dimerized stacks in contrast to radical cation salts of unsubstituted analogues BDT-TTP, which has a strong tendency to form uniform stacks. The results of band calculation indicate that TMEO-ST-TTP salts have effectively half-filled band and quasi-one-dimensional Fermi surface. Their metallic states are retained by large enough interstack interaction to suppress Peierls transition as well as small on-site Coulomb energy. Considering that the superconducting state is thought to lie between metal and antiferromagnetic Mott insulating state (4), slight modifications on TMEO-ST-TTP conductors are very promising to explore new superconductors. We are currently investigating on the synthesis of analogues of TMEO-ST-TTP, in which selenium atoms are exchanged or added to the other positions of sulfurs, as well as preparation of TMEO-ST-TTP salts with different anions.

ACKNOWLEDGMENTS

This work is partially supported by Grant-in-Aid for Scientific Research No. 09640687, 11640581 and 13440209 from the Ministry of Education, Science, Sports and Culture.

REFERENCES

1. Z. V. Vardeny and A. J. Epstein (Eds.), *in* Recent Proceedings of International Conferences: *Synth. Met.* **84–86** (1997); P. Bernier, S. Lefrant, and G. Bidan (Eds), *Synth. Met.* **101–103** (1999); H. Neugebauer (Ed.), *Synth. Met.* **119–121** (2001).
2. T. Ishiguro, K. Yamaji, and G. Saito, *in* "Organic Superconductors." 2nd edn. Springer-Verlag Berlin, Heidelberg, 1998; J. M. Williams, J. R. Ferraro, R. J. Thorn, K. D. Carlson, U. Geiser, H. H. Wang, A. M. Kini, and M.-H. Whangbo, "Organic Superconductors (Including Fullerenes) Synthesis, Structure, Properties and Theory," Prentice–Hall, Englewood Clifts, NJ, 1992.
3. J. Ferraris, D. O. Cowan, V. V. Walatka, and J. H. Perlstein, *J. Am. Chem. Soc.* **95,** 948 (1973); L. B. Coleman, J. A. Cohen, D. J. Sandman, F. G. Yamagishi, A. F. Garito, and A. J. Heeger, *Solid State Commun.* **12,** 1125 (1973); J. A. Cohen, L. B. Coleman, A. F. Garito, and A. J. Heeger, *Phys. Rev. B* **10,** 1298 (1974).
4. K. Kanoda, *Hyperfine Interact.* **104,** 235 (1997).
5. Y. Misaki, H. Nishikawa, K. Kawakami, S. Koyanagi, T. Yamabe, and M. Shiro, *Chem. Lett.* 2321 (1992); Y. Misaki, T. Matsui, K. Kawakami, H. Nishikawa, T. Yamabe, and M. Shiro, *Chem. Lett.* 1337 (1993).
6. Y. Misaki, H. Fujiwara, T. Yamabe, T. Mori, H. Mori, and S. Tanaka, *Chem. Lett.* 1653 (1994).
7. T. Mori, Y. Misaki, H. Fujiwara, and T. Yamabe, *Bull. Chem. Soc. Jpn.* **67,** 2685 (1994).
8. T. Mori, Y. Misaki, H. Fujiwara, T. Yamabe, H. Mori, and S. Tanaka, *Mol. Cryst. Liq. Cryst.* **284,** 271 (1996) and refrences therein.
9. Y. Misaki, K. Kawakami, H. Fujiwara, T. Miura, T. Kochi, M. Taniguchi, T. Yamabe, T. Mori, H. Mori, and S. Tanaka, *Mol. Cryst. Liq. Cryst.* **296,** 77 (1997).
10. Y. Misaki, T. Miura, M. Taniguchi, H. Fujiwara, T. Yamabe, T. Mori, H. Mori, and S. Tanaka, *Adv. Mater.* **9,** 714 (1997).
11. Y. Misaki, T. Kochi, T. Yamabe, and T. Mori, *Adv. Mater.* **10,** 588 (1998).
12. Y. Misaki, K. Tanaka, M. Taniguchi, T. Yamabe, T. Kawamoto, and T. Mori, *Chem. Lett.* 1249 (1999).
13. G. Saito, T. Enoki, K. Toriumi, and H. Inokuchi, *Solid State Commun.* **42,** 557 (1982).
14. T. Mori, H. Inokuchi, Y. Misaki, H. Nishikawa, T. Yamabe, H. Mori, and S. Tanaka, *Chem. Lett.* 2085 (1993).
15. Y. Misaki, H. Nishikawa, T. Yamabe, T. Mori, and H. Inokuchi, *Bull. Chem. Soc. Jpn.* **67,** 2368 (1994).
16. T. Mori, Y. Misaki, H. Nishikawa, T. Yamabe, H. Mori, and S. Tanaka, *Synth. Met.* **70,** 873 (1995).
17. Preliminary results on TMEO-ST-TTP and its radical cation salts have been reported in the following papers: (a) Y. Misaki, M. Taniguchi, K. Tanaka, K. Takimiya, A. Morikami, T. Otsubo, and Mori, *Chem. Lett.* 859 (1999); (b) Y. Misaki, T. Kaibuki, T. Monobe, K. Tanaka, M. Taniguchi, K. Tanaka, T. Yamabe, K. Takimiya, A. Morikami, T. Otsubo, and T. Mori, *Synth. Met.* **102,** 1781 (1999).
18. H. Anzai, J. M. Delrieu, S. Takasaki, S Nakatsuji, and J. Yamada, *J. Cryst. Growth* **154,** 145 (1995).
19. G. M. Sheldrick, C. Kruger, R. Goddard, *in* "Crystallographic Computing 3," p. 175 Oxford University Press, Oxford, 1985.
20. T. Mori, A. Kobayashi, Y. Sasaki, H. Kobayashi, G. Saito, and H. Inokuchi, *Bull. Chem. Soc. Jpn.* **57,** 627 (1984); T. Mori and M. Katsuhara, *J. Phys. Soc. Jpn.* **21,** 826 (2002).
21. V. F. Kaminskii, T. G. Prokhoroea, R. P. Shibaeva, and E. B. Yagubskii, *Pis'ma Eksp. Teor. Fiz.* **39,** 15 (1984); T. Mori, A. Kobayashi, G. Saito, and H. Inokuchi, *Chem. Lett.* 957 (1984); J. M. Williams, H. H. Wang, M. A. Beno, T. J. Emge, L. M. Sowa, P. T. Coops, F. Behroozi, L. N. Hall, K. D. Carlson, and G. W. Crabtree, *Inorg. Chem.* **23,** 3839 (1984).
22. T. Mori and H. Inokuchi, *J. Phys. Soc. Jpn.* **57,** 3674 (1988).
23. T. Komatsu, N. Matsukawa, T. Inoue, and G. Saito, *J. Phys. Soc. Jpn.* **65,** 1340 (1996).
24. The transfer integral (t) is defined by the following equation, $t = 10S$.
25. The difference between first and second redox potentials obtained from cyclic voltammetry in solution (0.23 V for TMEO-ST-TTP and 0.31 V for BEDT-TTF) occasionally suggests that on-site Coulomb energy of TMEO-ST-TTP is about two-thirds as large as that of BEDT-TTF.